180 USING PRACTICALLY PERFECT INTENSITY HINDCASTS TO IDENTIFY THE ENVIRONMENTS OF SIGNIFICANT SEVERE WEATHER OUTBREAKS

Andrew R. Wade*
Cooperative Institute for Severe and High-Impact Weather Research and Operations (CIWRO), Norman, OK

Israel L. Jirak
Storm Prediction Center, Norman, OK

Victor A. Gensini
Northern Illinois University, Dekalb, IL

Jacob Vancil
CIWRO, Norman, OK

1. INTRODUCTION

The National Weather Service Storm Prediction Center (SPC) defines "significant severe" thunderstorms as those producing tornado damage rated at least EF2 on the enhanced Fujita scale, hail at least 5 cm (2 in) in diameter, and/or straight-line winds of at least 33 m s^{-1} (75 mph). SPC's operational convective outlooks are based on probabilities of occurrence within 40 km (25 mi) of a point. Climatologies such as Evans and Doswell (2001), Thompson et al. (2003, 2007, 2012), Taszarek et al. (2020), and others have made the parameter spaces supporting significant severe weather reasonably well known. However, significant severe events range from lone reports marginally meeting criteria to rare, destructive, and deadly regional outbreaks. The difference in impacts is profound for significant tornado events; a small number of tornado days account for a large majority of casualties. To help forecasters and stakeholders anticipate extreme local impacts with longer lead time, it is essential to identify signals for these outlier events.

The meteorological differences between isolated significant severe events and high-end outbreaks are not well established. Compared to isolated events, are significant severe outbreaks characterized by more favorable values of operationally identifiable bulk environmental parameters, similarly favorable values present over a wider area, or neither? Do outbreaks occur in synoptic settings much like those of isolated significant severe, or are there differences that favor more widespread severe storms? To answer these questions, this study quantifies the mesoscale coverage of thousands of significant severe weather events and relates it to bulk parameters from operational objective analyses.

*Corresponding author: Andrew R. Wade, andrew.wade@noaa.gov

2. DATA AND METHODS

2.1 *Practically perfect hindcasts and outbreaks*

Practically perfect hindcasts (PPHs; Hitchens et al. 2013, Gensini et al. 2020) covering the contiguous U.S. are produced from distributions of severe reports to approximate ideal SPC outlooks given predictability limits. Significant severe PPHs imply that one isolated report does not quite warrant a 10 percent hatched contour at all, while major outbreaks exceed that threshold by a factor of two or more. While the standard method of constructing PPHs is widely accepted and directly tied to the scale of coverage that SPC forecasts, it does depend on the availability and accuracy of storm reports, and cannot represent dense sub-grid-scale concentrations of reports.

This study defines outbreaks of each significant severe hazard as the top decile of nonzero maximum daily PPH probabilities over the analysis period, 1 January 2007–31 December 2021, using the 12 UTC–12 UTC convective day. This arbitrary definition of 'outbreak' is

restrictive and is not intended for other applications. However, it is as objective as possible and proves effective at identifying a subset of dangerous high-end tornado events. The top decile of significant tornado days—four days a year on average, and only 2.5 percent of all U.S. tornado days—accounted for 75 percent of direct tornado fatalities, 65 percent of direct tornado injuries, and 50 percent of tornado property damage over the analysis period. (Omitting the 27 April 2011 outlier reduces the fraction of fatalities to 64 percent.) The average frequency of significant tornado outbreaks by this definition, four or five days a year, corresponds to the ideal frequency of "double hatching" in SPC's experimental conditional intensity forecasts (e.g., Clark et al. 2021), while wind and hail "outbreaks" are more common.

2.2 *Storm environment data and compositing*

The environmental fields used in this study are drawn from SPC's SFCOA archive (Bothwell et al. 2002). Once the gridpoint of the daily maximum PPH probability is found, a peak time must be determined. PPHs over three-hour periods beginning on each hour from 12 UTC to 09 UTC during the convective day are used to define a three-hour peak window at the daily maximum gridpoint, and the environment is sampled one hour into the three-hour peak window. The results do not appear very sensitive to minor variations in peak time definition. To avoid sampling environments that would not support deep convection, each environment added to a composite must have at least 100 J kg^{-1} CAPE (MLCAPE for tornadoes, MUCAPE for hail and wind) at its center point. In a small minority of cases, the center point is shifted up to three gridpoints south and/or east of the daily maximum PPH to obtain adequate CAPE. If this search fails, the case is excluded from the composite; this affects a negligible number of events, including no tornado outbreaks. Additionally, some SFCOA fields, such as CAPE within specific layers, CIN, and certain combined indices, are not defined where CAPE is zero. Undefined data points are not included in compositing. Thus, some gridpoints in these composite fields, especially those far from the center, represent the mean of fewer environments than the number of days in the sample. This does not have any meaningful effect except for some noise in mean CIN fields away from the center of the composites.

3. RESULTS

3.1 *Significant severe PPH climatology*

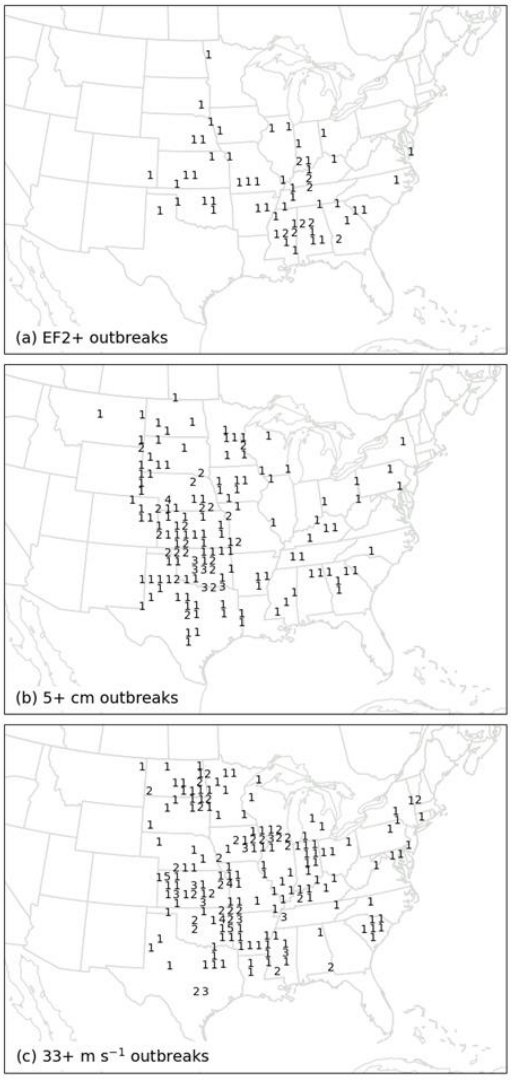

Fig. 1. Total significant (a) tornado, (b) hail, and (c) wind outbreaks centered at each 80-km gridpoint, 2007–2021 (inclusive).

Most significant tornado days and significant wind days, and a large minority of significant hail days, have a maximum PPH probability of 7 percent, which corresponds to an isolated grid cell containing significant severe. This means that existing climatologies of significant severe heavily weight such isolated occurrences,

offering further motivation to narrow in on the parameter spaces of outbreaks. In the following sections, days with a maximum PPH probability of 7 percent are labeled as the “isolated” subset. Fig. 1 depicts the spatial distribution of PPH maxima corresponding to significant severe outbreaks on the 80-km PPH grid. This climatology is roughly in line with the 10 percent PPH significant severe climatology in Gensini et al. (2020). The size of each subset of events is given in the panel labels in Fig. 2 below.

3.2 *Synoptic settings of significant severe outbreaks*

Unsurprisingly, the composite environments of all significant severe outbreaks feature a 500-hPa trough axis just west of the event, a surface low near or north of the event, and a plume of high near-surface equivalent potential temperature extending from south to north into the event area (Fig. 2). The midlevel height gradient in the EF2+ outbreak composite is notably larger than in even the other outbreak composites; this is associated with the kinematic characteristics described in section 3.3 below.

3.3 *Mesoscale ingredients of significant severe outbreaks*

Significant tornado outbreaks tend to occur with slightly less MLCAPE, slightly lower MLLCLs, much larger 0–6-km bulk shear, and much larger SRH over both 0–1-km and 0–3-km layers (0–1-km shown) than isolated significant tornadoes (Fig. 3). These differences in the kinematic

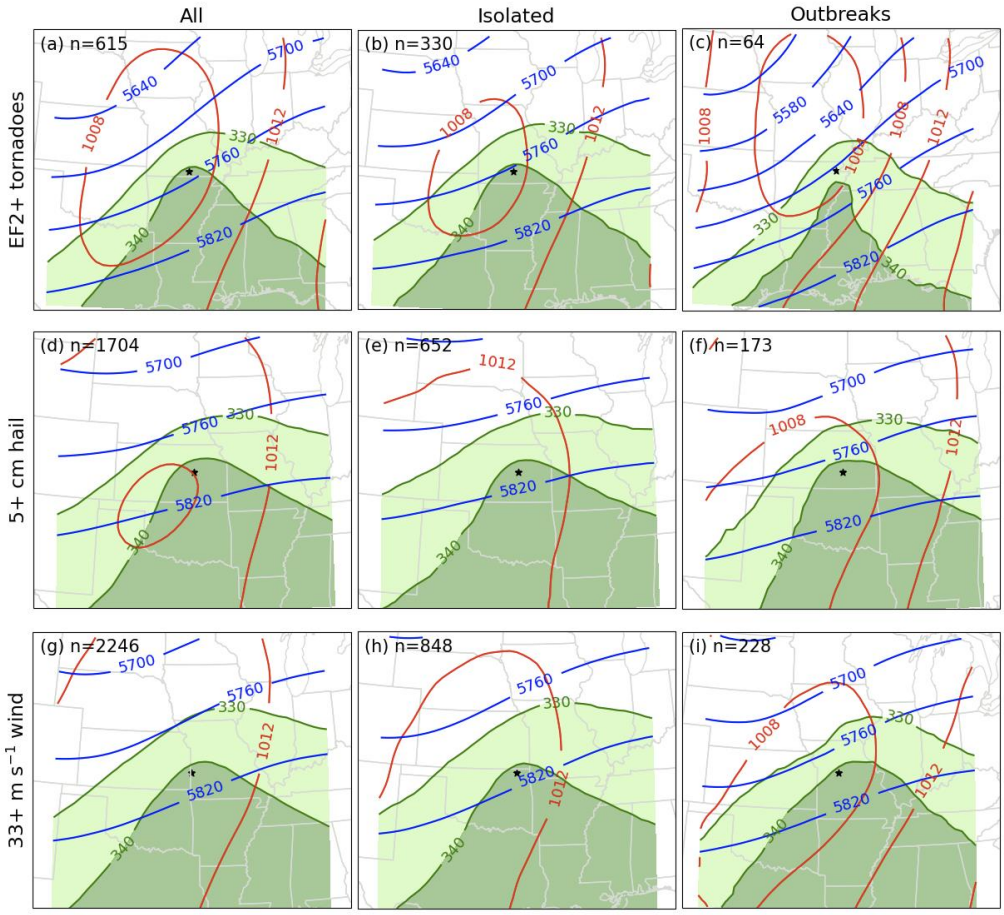

Fig. 2. Composite 500-hPa height (m; blue contours), mean sea level pressure (hPa; red contours), and 2-m equivalent potential temperature (K; green contours and shading) of significant severe events, with the number of composited events given in each panel. Stars denote composite centers (maximum PPH gridpoints).

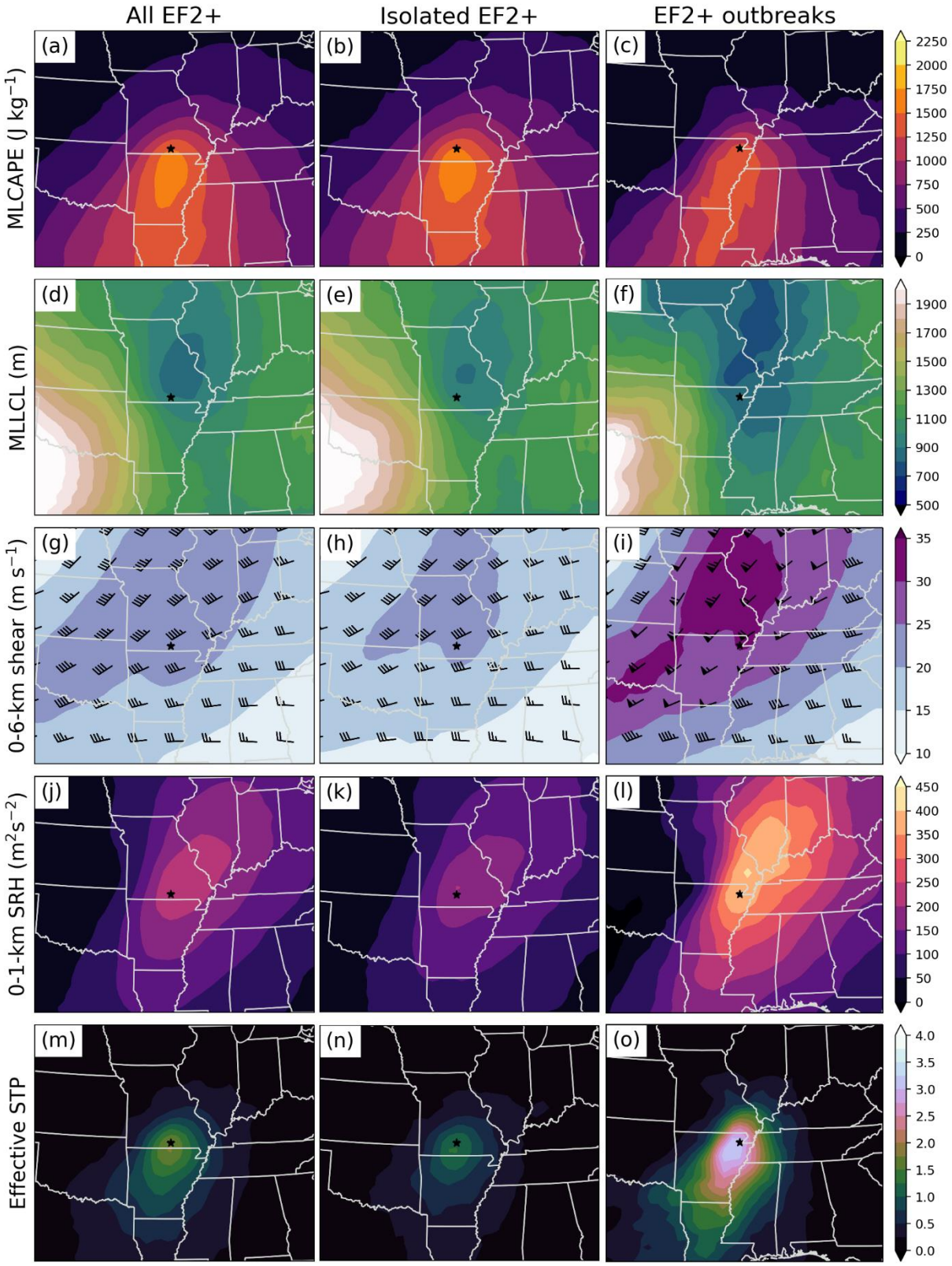

Fig. 3. Composite (a–c) MLCAPE, (d–f) MLLCL, (g–i) 0–6-km bulk shear, (j–l) 0–1-km SRH, and (m–o) STP in (left to right) all significant tornado events, isolated significant tornado events, and significant tornado outbreaks. Full barbs in panels (g–i) represent 5.1 m s^{-1} (10 kt); pennants represent 25.7 m s^{-1} (50 kt).

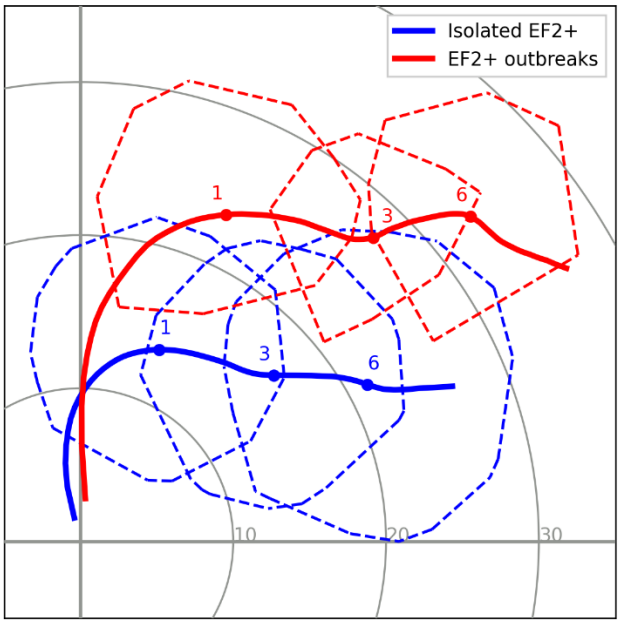

Fig. 4. Composite RUC/SFCOA hodographs for the isolated significant tornado (blue) and significant tornado outbreak (red) composites. Winds/rings are in m s^{-1}. Dashed polygons around the 1, 3, and 6 km points are the convex hulls of the 50 percent of points nearest to the mean at those levels. Hodographs end at 10 km AGL.

fields dominate the effective-layer significant tornado parameter (STP; Thompson et al. 2003, 2007) so that it is much larger in the outbreak composite (Fig. 3o).

The contrasting environmental kinematic fields of isolated significant tornadoes and outbreaks are further illuminated by composite hodographs (Fig. 4). Hodographs are drawn from the center point of each member of the two-dimensional composite environments in Fig. 3 at the same peak time. SFCOA supplies 10-m winds at the lowest point of each hodograph, and data above 10 m are Rapid Update Cycle (RUC) model analyses archived on pressure levels at 25-hPa intervals. These individual hodographs are composited using the method described by Parker (2014). While the shapes of the hodographs are qualitatively similar—clockwise-turning segments up to 1–1.5 km becoming mostly straight above—flow is substantially stronger throughout the depth of the outbreak composite.

Furthermore, the difference in STP distributions/interquartile ranges between isolated EF2+ events and EF2+ outbreaks (Fig. 5) is comparable to the difference between significantly tornadic and nontornadic storms in Thompson et al. (2003) Fig. 18. However, it must be noted that because isolated significant tornado days (n = 330) are so much more common than significant tornado outbreaks (n = 64), STP values near the center of the outbreak distribution are still associated with more isolated events than outbreaks.

Among significant hail (Fig. 6) and wind (Fig. 7) events, mesoscale ingredients discriminate somewhat less well between outbreaks and isolated occurrences. Contrary to its relationship to tornado outbreaks, larger CAPE seems to favor more widespread significant hail and wind. Stronger deep-layer shear also appears in both outbreak composites. Two of the relevant combined indices archived from SFCOA are the significant hail parameter (SHIP; SPC 2022a) and derecho composite parameter

(DCP; SPC 2022b). SHIP ranges from below 1 near the isolated 5+ cm hail center point (Fig. 6h) to about 1.75 in the outbreak composite (Fig. 6i). DCP maxima slightly south of the composite centers vary from less than 2 in the isolated significant wind composite (Fig. 7h) to greater than 4 in the outbreak composite (Fig. 7i).

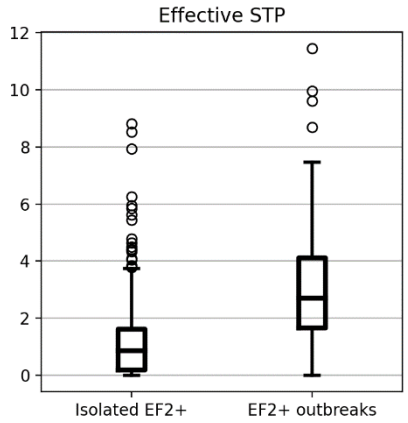

Fig. 5. Boxplots of STP distributions at the center points of the isolated significant tornado and significant tornado outbreak composites.

4. DISCUSSION

The most immediate application of these composite environments and point distributions of parameters is in anticipating significant tornado outbreaks. The primary difference between isolated occurrences and outbreaks of significant tornadoes clearly lies in the meso-β- and meso-α-scale wind field. The greatest relative difference in a single parameter is in SRH, whose maximum is roughly twice as large in the outbreak composite as in the isolated composite. 0–1-km SRH near the center of the outbreak composite exceeds the 90th percentile of values associated with all EF2+ tornadoes in Thompson et al. (2003). While some climatological work (Coffer et al. 2020) has emphasized layers as near as possible to the surface in calculating SRH for tornado forecasting, Coniglio and Parker's (2020) analysis of near-storm radiosonde observations also found larger SRH and storm-relative flow over deeper layers near tornadic supercells than nontornadic ones. In this sample, 0–3-km SRH (not shown) behaves almost identically to 0–1-km SRH in its spatial distribution and in the relative difference between outbreaks and isolated EF2+. 0–6-km bulk shear is also much greater in the EF2+ outbreak composite than in any of the other composites for any hazard. Using these real-world environments alone (without, e.g., idealized modeling), it is probably not possible to disentangle the roles of multiple kinematic parameters over different layers, as all describe a relatively strong, amplified upper wave and pronounced low-level response contributing to a highly distinctive mean hodograph throughout the troposphere (Fig. 4).

Markowski et al. (1998) documented large heterogeneity in observed SRH on scales < 100 km in a few Great Plains cases and hypothesized that this could explain variability in tornado production among storms that appear to share a mesoscale environment. The SRH values found in the outbreak composite allow a wide margin for such heterogeneity without inflow ever becoming unfavorable for significant tornadoes. In the idealized simulations of Coffer and Parker (2017), the base state with larger SRH generated storms that consistently became tornadic with little sensitivity to random perturbations, while the base state with smaller SRH produced a variety of nontornadic and weakly tornadic storms in response to perturbations. Similarly, Markowski (2020) simulated an ensemble of idealized supercells in a favorable tornadic environment with small random temperature perturbations in the boundary layer, and while large variability in vortex intensity and timing resulted, all storms produced vortices classified as tornadic despite 0–1-km SRH more than 100 m2 s-2 smaller than at the center of the outbreak composite. In view of the typical significant tornado outbreak parameter space shown here, it is at least plausible that values of SRH beyond those tested in such simulations can even further reduce sensitivity of tornado production to typical environmental heterogeneity and stochastic intrastorm processes.

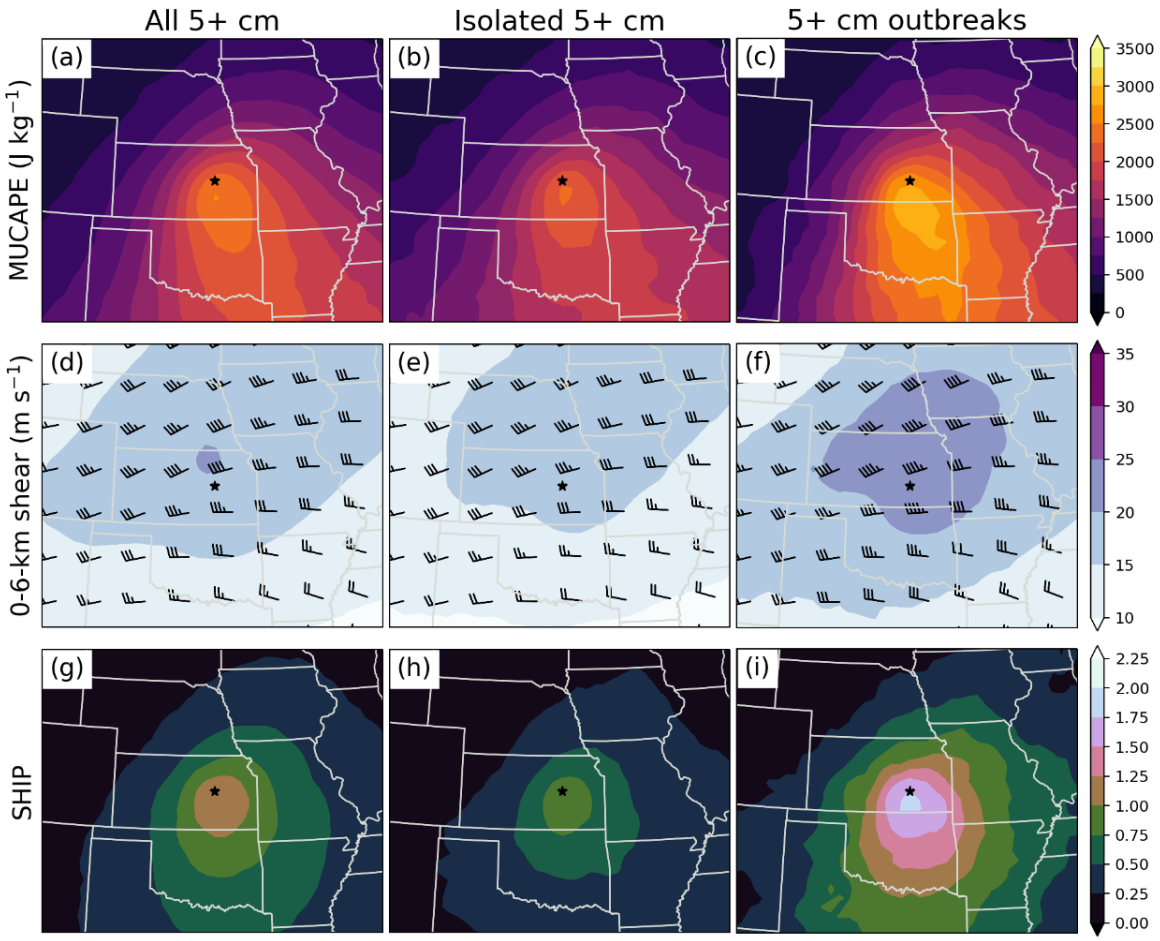

Fig. 6. Composite (a–c) MUCAPE, (d–f) 0–6-km bulk shear, and (j–l) SHIP in (left to right) all significant hail events, isolated significant hail events, and significant hail outbreaks. Wind barbs are as in Fig. 3.

5. SUMMARY

Dense outbreaks of several EF2+ tornadoes usually occur amid much larger deep-layer shear and low-level SRH than isolated EF2+ tornadoes (or any other type of significant severe event). Combined with a subtler tendency toward lower LCLs, this yields much larger mean and median values of STP in outbreaks. The composited values of SRH and STP across 64 outbreaks greatly surpass the thresholds already known to support significant tornadoes in general. This key result should be adopted for operational consideration given the disproportionate impacts of the outbreak set. More analysis is needed to determine primary limiting factors in the many isolated significant tornado events with bulk parameter spaces supportive of outbreaks.

Regarding the other severe hazards, higher values of SHIP and DCP associated with outbreaks of significant hail and wind, respectively, support these parameters' operational utility for quickly identifying significant severe environments. However, attribution to individual ingredients of the combined indices is not as simple as in the case of tornadoes; thermodynamic and kinematic components both play notable roles. Ongoing work separates warm- and cool-season significant severe events. Automated tracking of mesoscale convective systems is being developed to create similar composites for systems that meet various severity criteria, up to and including derechos, further informing SPC's development of conditional intensity products.

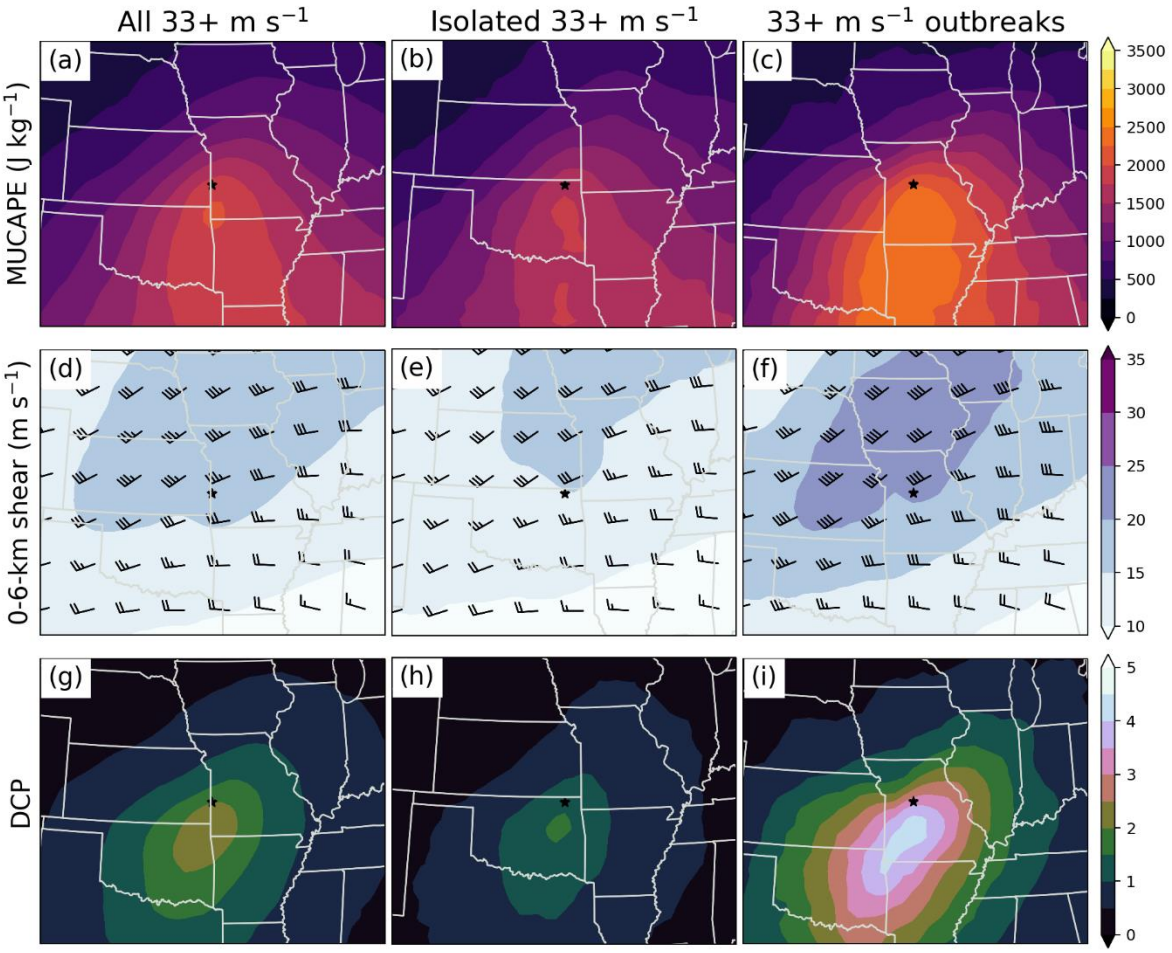

Fig. 7. Composite (a–c) MUCAPE, (d–f) 0–6-km bulk shear, and (j–l) DCP in (left to right) all significant wind events, isolated significant wind events, and significant wind outbreaks. Wind barbs are as in Fig. 3.

REFERENCES

Clark, A. J., and Coauthors, 2021: Spring Forecasting Experiment 2021: Preliminary findings and results . NOAA Hazardous Weather Testbed, NOAA, 86 pp., https://hwt.nssl.noaa.gov/sfe/2021/docs/HWT_SFE_2021_Prelim_Findings_FINAL.pdf.

Coffer, B. E., M. D. Parker, J. M. Dahl, L. J. Wicker, and A. J. Clark, 2017: Volatility of tornadogenesis: an ensemble of simulated nontornadic and tornadic supercells in VORTEX2 environments. *Mon. Wea. Rev.*, **145**, 4605–4625, https://doi.org/10.1175/MWR-D-17-0152.1.

Coffer, B. E., M. Taszarek, and M. D. Parker, 2020: Near-ground wind profiles of tornadic and nontornadic environments in the United States and Europe from ERA5 reanalyses. *Wea. Forecasting*, **35**, 2621–2638, https://doi.org/10.1175/WAF-D-20-0153.1.

Coniglio, M. C., and M. D. Parker, 2020: Insights into supercells and their environments from three decades of targeted radiosonde observations. *Mon. Wea. Rev.*, **148**, 4893–4915, https://doi.org/10.1175/MWR-D-20-0105.1.

Evans, J. S., and C. A. Doswell III, 2001: Examination of derecho environments using proximity soundings. *Wea. Forecasting*, **16**, 329–342, https://doi.org/10.1175/1520-0434(2001)016<0329:EODEUP>2.0.CO;2.

Gensini, V. A., A. M. Haberlie, and P. T. Marsh, 2020: Practically perfect hindcasts of severe convective storms. *Bull. Amer. Meteor. Soc.*, **101**, E1259–E1278, https://doi.org/10.1175/BAMS-D-19-0321.1.

Hitchens, N. M., H. E. Brooks, and M. P. Kay, 2013: Objective limits on forecasting skill of rare events. *Wea. Forecasting*, **28**, 525–534, https://doi.org/10.1175/WAF-D-12-00113.1.

Markowski, P. M., J. M. Straka, E. N. Rasmussen, and D. O. Blanchard, 1998: Variability of storm-relative helicity during VORTEX. *Mon. Wea. Rev.*, **126**, 2959–2971, https://doi.org/10.1175/1520-0493(1998)126<2959:VOSRHD>2.0.CO;2.

Markowski, P. M., 2020: What is the intrinsic predictability of tornadic supercell thunderstorms? *Mon. Wea. Rev.*, **148**, 3157–3180, https://doi.org/10.1175/MWR-D-20-0076.1.

Parker, M. D., 2014: Composite VORTEX2 supercell environments from near-storm soundings. *Mon. Wea. Rev.*, **142**, 508–529, https://doi.org/10.1175/MWR-D-13-00167.1.

SPC, cited 2022: Significant hail parameter (SHIP), http://www.spc.noaa.gov/exper/mesoanalysis/help/help_sigh.html.

SPC, cited 2022: Derecho composite parameter (DCP), http://www.spc.noaa.gov/exper/mesoanalysis/help/help_DCP.html.

Taszarek, M., J. T. Allen, T. Púčik, K. Hoogewind, and H. E. Brooks, 2020: Severe convective storms across Europe and the United States. Part II: ERA5 environments associated with lightning, large hail, severe wind and tornadoes. *J. Climate*, **33**, 10263–10286, https://doi.org/10.1175/JCLI-D-20-0346.1.

Thompson, R. L., R. Edwards, J. A. Hart, K. L. Elmore, and P. Markowski, 2003: Close proximity soundings within supercell environments obtained from the Rapid Update Cycle. *Wea. Forecasting*, **18**, 1243–1261, https://doi.org/10.1175/1520-0434(2003)018<1243:CPSWSE>2.0.CO;2.

Thompson, R. L., C. M. Mead, and R. Edwards, 2007: Effective storm-relative helicity and bulk shear in supercell thunderstorm environments. *Wea. Forecasting*, **22**, 102–115, https://doi.org/10.1175/WAF969.1.

Thompson, R. L., B. T. Smith, J. S. Grams, A. R. Dean, and C. Broyles, 2012: Convective modes for significant severe thunderstorms in the contiguous United States. Part II: Supercell and QLCS tornado environments. *Wea. Forecasting*, **27**, 1136–1154, https://doi.org/10.1175/WAF-D-11-00116.1.